

# Niğde Ömer Halisdemir Üniversitesi Mühendislik Bilimleri Dergisi Niğde Ömer Halisdemir University Journal of Engineering Sciences

Araştırma makalesi / Research article





# Multi-scale remote sensing of desertification trends and climate-vegetation interactions in the Konya basin, Türkiye (2000–2025)

Konya havzası, Türkiye'de çölleşme eğilimleri ve iklim-bitki örtüsü etkileşimlerinin çok ölçekli uzaktan algılama analizi (2000–2025)

# Ahmet Emin Karkınlı<sup>1,\*</sup>

<sup>1</sup> Niğde Ömer Halisdemir University, Geomatics Engineering Department, 51240, Niğde, Türkiye

#### Abstract

Konya Basin, a key agro-ecosystem in Turkey, is increasingly vulnerable to desertification. This study assesses vegetation dynamics and climatic drivers between 2000 and 2025 using the Google Earth Engine platform. MODIS time-series (NDVI and SAVI) were analyzed to map long-term trends, and medium-resolution Landsat data identified degradation hotspots. Our results reveal an apparent contradiction. The basin shows a subtle greening trend, particularly in croplands (+0.0042 NDVI units yr<sup>-1</sup>). However, medium-resolution Landsat data simultaneously indicate degradation hotspots covering a total of 3471.93 km<sup>2</sup>. Croplands account for 21.4% of these areas, and about 70% occur below 1000 m, where groundwater-dependent irrigation is most intense. Climatic drivers clarify this dynamic. A significant warming trend of 0.05 °C yr<sup>-1</sup> (p = 0.0102) was detected, while vegetation correlated positively with precipitation (r = 0.50, p < 0.01) but showed no significant relationship with temperature (r = 0.09, p =0.66). Spatial maps confirmed precipitation control in northern rainfed grasslands and temperature stress in irrigated southern plains. This multi-scale approach shows that basin-wide averages can be misleading, as modest greening coexists with local degradation. The findings emphasize the need for spatially explicit data to guide targeted land and water management policies to mitigate desertification risks in this vital region.

**Keywords:** Desertification, Remote sensing, NDVI/SAVI, Climate-vegetation relationships, Hotspot analysis

# 1 Introduction

Desertification, defined as land degradation in arid, semiarid, and dry sub-humid areas resulting from climatic variations and human activities, poses a critical threat to global food security, biodiversity, and ecosystem services [1]. The IPCC estimates that desertification affects over 2.7 billion people worldwide, with semi-arid regions particularly vulnerable due to their sensitivity to climate change and land-use pressures [2]. Covering ~40% of Earth's land Öz

Türkiye'nin önemli bir agro-ekosistemi olan Konya Havzası, çölleşmeye karşı giderek daha savunmasız hale gelmektedir. Bu çalışma, Google Earth Engine platformu kullanılarak 2000 ve 2025 yılları arasındaki bitki örtüsü dinamiklerini ve iklimsel etkenleri değerlendirmektedir. Uzun vadeli eğilimleri haritalamak için MODIS zaman serileri (NDVI ve SAVI) analiz edilmiş ve orta çözünürlüklü Landsat verileriyle bozulma odak noktaları belirlenmiştir. Bulgularımız bir çelişkiyi koymaktadır; zira havza, özellikle tarım arazilerinde (+0.0042 NDVI birimi/yıl) hafif bir yeşillenme eğilimi gösterirken, Landsat verileri toplam 3471.93 km² alana yayılan bozulma odakları olduğunu göstermektedir. Bu alanların %21.4'ünü tarım arazileri oluşturmakta ve yaklaşık %70'i, yeraltı suyuna dayalı sulamanın en yoğun olduğu 1000 m'nin altındaki rakımlarda meydana İklimsel gelmektedir. etkenler bu dinamiği netleştirmektedir. Anlamlı bir ısınma eğilimi (0.05 °C/yıl; p = 0.0102) tespit edilirken, bitki örtüsü yağışla pozitif korelasyon göstermiş (r = 0.50, p < 0.01) ancak sıcaklıkla anlamlı bir ilişki sergilememiştir (r = 0.09, p = 0.66). Mekansal haritalar, kuzeydeki yağışa bağımlı otlaklarda yağış kontrolünü ve güneydeki sulu tarım ovalarında sıcaklık stresini doğrulamıştır. Bu çok ölçekli yaklaşım, mütevazı bir yeşillenmenin yerel bozulmayla bir arada bulunması nedeniyle havza geneli ortalamalarının yanıltıcı olabileceğini göstermektedir. Bulgular, bu hayati bölgedeki cöllesme risklerini azaltmak için hedefe yönelik arazi ve su vönetimi politikalarına rehberlik edecek mekansal olarak ayrıntılı verilere duyulan ihtiyacı vurgulamaktadır.

**Anahtar kelimeler:** Çölleşme, Uzaktan algılama, NDVI/SAVI, İklim-vejetasyon ilişkileri, Hotspot analizi

surface, these regions face rising temperatures, erratic precipitation, and human-induced pressures like overgrazing and intensive agriculture, leading to soil erosion, productivity decline, and ecosystem resilience loss [3]. Remote sensing has become indispensable for monitoring such vast areas, with vegetation indices like NDVI and SAVI (reducing soil background effects in sparse vegetation; [4]) widely used to track dynamics and detect hotspots. Global studies consistently link these indices to climatic factors, for

<sup>\*</sup> Sorumlu yazar / Corresponding author, e-posta / e-mail: akarkinli@ohu.edu.tr (A. E. Karkınlı) Geliş / Received: 26.09.2025 Kabul / Accepted: 07.10.2025 Yayımlanma / Published: 15.10.2025 doi: 10.28948/ngumuh.1791557

example, NDVI-precipitation correlations in Central Asia [5], temperature-driven land cover shifts, such as biome replacements in Mediterranean mountains [6], and NDVI-LST associations in Saudi Arabia [7], revealing greening—degradation contradictions in Argentina [8], Iraq [9], Australia [10], the Sahel [11], and China [12, 13].

The Konya Basin, a semi-arid closed basin in central Turkey, mirrors these global dynamics. Covering ~50,000 km2, it is one of the country's most important grainproducing regions, yet is increasingly threatened by drought, soil erosion, and groundwater depletion [14]. Remote sensing studies highlight its vulnerability: long-term warming trends of +1-2 °C have been linked to vegetation stress (~10-15%) [15]; DInSAR analyses revealed land subsidence of up to 5 cm/year due to aquifer over-extraction [16]; MODIS- and index-based drought monitoring indicates increasing frequency and severity of drought events in the Konya Basin in recent decades [17]; furthermore, recent significant intensification analyses confirm a meteorological, hydrological, and especially groundwater drought across the basin, directly linking it to unsustainable water management practices [18]; long-term Landsat analyses report substantial reductions (~20-25%) in lentic system surface areas [19]; these hydrological changes have been directly associated with increased water abstraction for agriculture, leading to severe consequences such as rising salinity in lakes and the loss of critical waterbird and fish populations [20]; and Sentinel-1 SAR time-series studies demonstrate clear links between crop backscatter dynamics and reduced vegetation vigor during drought years [21]. These findings confirm the basin's susceptibility to desertification but remain fragmented in scope.

Despite these contributions, a research gap persists in integrating multi-sensor and multi-scale data for a holistic assessment of land degradation in the Konya Basin over recent decades [22, 23]. Previous work has focused on single drivers or scales, without systematically investigating whether apparent greening trends at the basin level mask localized degradation hotspots. This gap is critical, as aggregate NDVI averages can obscure spatial heterogeneity and fail to inform targeted interventions [24, 25]. International examples illustrate the importance of multiapproaches for disentangling climatic anthropogenic contributions: Central Asia [25], the Sahel [11], and Iran [26]. Global assessments also suggest that roughly 20-30% of degradation is linked to human activities [27]. These findings highlight the need for a basin-scale framework in Konya that explicitly separates climatic variability from human drivers.

This study addresses this gap by conducting a comprehensive, multi-scale analysis of vegetation dynamics in the Konya Basin from 2000 to 2025. Specifically, we aim to: (1) quantify long-term spatial—temporal trends in vegetation health using MODIS-derived NDVI and SAVI; (2) analyze their relationships with precipitation and temperature; and (3) identify medium-resolution (30 m) degradation hotspots using Landsat data and evaluate their distribution across land cover types. By integrating macroscale (MODIS) and micro-scale (Landsat) analyses, this

research offers a novel perspective on desertification drivers and provides a robust evidence base for sustainable land and water management policies in one of Turkey's most vital agricultural regions.

# 2 Materials and Methods

# 2.1 Study Area

This study focuses on the Konya Closed Basin, a semiarid agro-ecosystem in the Central Anatolia region of Turkey (Figure 1; 38°-39° N, 32°-33° E). Covering approximately 50,000 km<sup>2</sup>, the basin is one of the country's most significant agricultural regions, primarily for grain production, with annual precipitation averaging 300-400 mm and a continental climate featuring hot, dry summers. The analysis was defined for the primary growing season (April-September) to capture vegetation dynamics during its most active phase. According to the ESA WorldCover dataset (2020), the basin's land cover is dominated by cropland (~60%), followed by grassland (~25%) and bare/sparse vegetation (~10%). Topographically, a significant portion of agricultural activity is concentrated in the plains at elevations below 1000 m, which are also most susceptible to environmental pressures such as groundwater depletion and soil erosion [22, 28, 29]

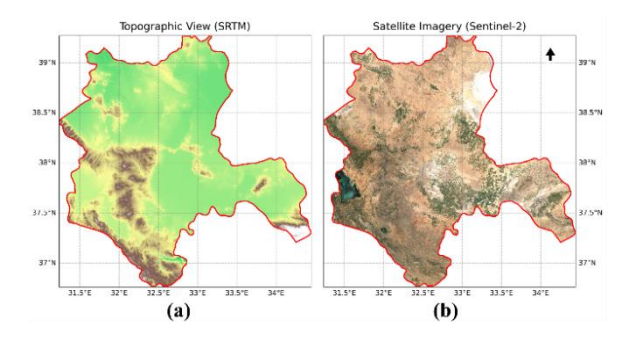


**Figure 1.** The study area, Konya Basin, showing (a) the topographic context from the SRTM Digital Elevation Model and (b) a true-color Sentinel-2 satellite composite

# 2.2 Data Acquisition

All remote sensing and climate data were acquired and processed using the Google Earth Engine (GEE) cloud computing platform [30]. The datasets used in this study are summarized in Table 1. For long-term vegetation trend analysis (2000-2025), we used the MODIS Terra/Aqua 16-Day L3 Global 250m product (MOD13Q1) for NDVI at 250 m resolution and the 8-Day L3 Global 500m Surface Reflectance product (MOD09A1) at 500 m resolution to calculate SAVI [31]. Medium-resolution hotspot analysis (2013-2025) was conducted using Landsat 8/9 Level 2, Collection 2, Tier 1 data at 30 m resolution [32]. Climatic variables were derived from the Climate Hazards Group InfraRed Precipitation with Station data (CHIRPS) daily dataset at 0.05° (~5 km) resolution for precipitation [33] and the ERA5-Land daily aggregated dataset at 0.1° (~11 km) resolution for mean 2-meter air temperature [34]. Land cover and topographic analysis was supported by the 2020 ESA WorldCover 10m land cover map [35] and the 30m SRTM Digital Elevation Model [36].

<b>Table 1.</b> Summary of datasets used in the study.	Table 1.	Summary	of datasets	used in	the study.
--	----------	---------	-------------	---------	------------

Data Type	Dataset Name / Source	Spatial Resolution	Temporal Resolution	Period	Purpose
Vegetation Index (NDVI)	MODIS/061/MOD13Q1	250 m	16-day	2000-2025	Long-term trend analysis
Vegetation Index (SAVI)	MODIS/061/MOD09A1	500 m	8-day	2000-2025	Long-term trend analysis
Medium-Res Vegetation	LANDSAT/LC08/C02/T1_L2	30 m	16-day	2013-2025	Hotspot detection
Precipitation	UCSB-CHG/CHIRPS/DAILY	~5.5 km	Daily	2000-2025	Climate correlation analysis
Temperature	ECMWF/ERA5_LAND/DAILY_AGGR	~11 km	Daily	2000-2025	Climate correlation analysis
<b>Land Cover</b>	ESA/WorldCover/v100	10 m	2020 (static)	2020	Stratification of results
Elevation	USGS/SRTMGL1_003	30 m	Static	N/A	Contextual analysis

# 2.3 Data Processing

We performed data preprocessing to generate analysisready annual time-series for the growing season. MODIS products underwent rigorous quality control using their respective Quality Assessment (QA) bands (SummaryQA for MOD13Q1 and StateQA for MOD09A1) to mask pixels contaminated by clouds, aerosols, or poor-quality observations (e.g., SummaryQA.eq(0)). The Normalized Difference Vegetation Index (NDVI) was calculated using the surface reflectance ( $\rho$ ) values of the Near-Infrared (NIR) and Red bands, as given in Equation 1 [37]:

$$NDVI = \frac{(\rho_{NIR} - \rho_{Red})}{(\rho_{NIR} + \rho_{Red})}$$
(1)

To account for soil background effects in sparsely vegetated areas, the Soil-Adjusted Vegetation Index (SAVI) was also calculated using Equation 2 [4]:

$$SAVI = \frac{(\rho_{NIR} - \rho_{Red})}{(\rho_{NIR} + \rho_{Red} + L)} \times (1 + L)$$
 (2)

where L is a soil adjustment factor, set to 0.5 for semiarid regions. Similarly, Landsat 8/9 data were masked for clouds using the QA\_PIXEL band before NDVI calculation. For all datasets, annual composites were created for each year from 2000 to 2025 by calculating the mean (for NDVI, SAVI, temperature) or sum (for precipitation) of all highquality observations within the April–September growing season. Processing used a 250 m scale and 1e13 maxPixels limit to ensure computational efficiency.

# 2.4 Trend and Correlation Analysis

We applied pixel-wise linear regression to the 26-year time-series of annual MODIS-derived NDVI and SAVI composites to quantify the rate and direction of vegetation change (e.g., NDVI units per year). The slope ( $\beta$ ) was calculated as given in Equation 3:

$$\beta = \frac{\sum (x_i - \overline{x})(y_i - \overline{y})}{\sum (x_i - \overline{x})^2}$$
 (3)

where  $x_i$  is time (years 2000-2025) and  $y_i$  is NDVI/SAVI, with significance tested at  $\alpha$ =0.05 [38]. To investigate

vegetation-climate relationships, pixel-wise Pearson's correlation was conducted between annual NDVI/SAVI and precipitation/temperature composites. The correlation coefficient (r) was computed as given in Equation 4:

$$r = \frac{\sum (x_{i} - \bar{x})(y_{i} - \bar{y})}{\sqrt{\sum (x_{i} - \bar{x})^{2} \sum (y_{i} - \bar{y})^{2}}}$$
(4)

with p-values for significance (p<0.05). Analysis was stratified by land cover class using the ESA WorldCover map to assess variations across cropland, grassland, and bare/sparse vegetation [35].

# 2.5 Medium-Resolution Hotspot Analysis

To identify areas of recent, severe degradation, a hotspot analysis was performed using the 30m resolution Landsat 8/9 data. A continuous NDVI change map ( $\Delta$ NDVI) was created by subtracting the mean growing season NDVI of an early period (2013–2015) from that of a late period (2023–2025), as given in Equation 5:

$$\Delta NDVI = NDVI_{late} - NDVI_{early}$$
 (5)

Based on the statistical distribution of this change map, a data-driven threshold was established at the 10th percentile of all negative change values (-0.0885) to classify pixels undergoing significant degradation as "hotspots" [38]. Hotspot areas were calculated in km² and stratified by land cover class (ESA WorldCover) and elevation (SRTM) to quantify human activity impacts, with significance tested at  $\alpha$ =0.05.

# 2.6 Statistical Validation

The statistical significance of the basin-wide temporal trends and correlations was calculated in Python from the exported summary CSV file. Linear regression was used to determine the p-value for the long-term temperature trend. Pearson's correlation coefficient (r), as defined in Equation 4, was used to assess the strength and significance of the relationships between annual vegetation indices and climatic variables. The significance of the correlation coefficient was tested using a t-statistic as given in Equation 6:

$$t = \frac{r\sqrt{n-2}}{\sqrt{1-r^2}}\tag{6}$$

Several sources of uncertainty were identified and acknowledged in this study. The primary source is the spatial resolution mismatch between the datasets used: moderateresolution vegetation (250-500 m), coarse-resolution climate data (~5–11 km), and high-resolution land cover (10 m) and hotspot (30 m) data. This was addressed by aggregating summary statistics for basin-wide analysis and by acknowledging this limitation in the interpretation of pixel-level results. A second source of uncertainty is the use of a static 2020 land cover map for stratifying trends over a 26-year period, which does not account for potential land use conversions. Finally, the medium-resolution hotspot analysis was constrained by the temporal availability of Landsat 8/9 data (post-2013), limiting a longer-term historical comparison of degradation at this scale. These limitations were considered during the discussion of the results.

## 3 Results and Discussion

# 3.1 Long-Term Temporal Trends and Climatic Relationships

The basin-wide temporal analysis for the growing season (April–September) from 2000 to 2025 reveals distinct trends in key environmental variables. As illustrated in Figure 2, both mean NDVI and SAVI exhibit a gradual increasing trend over the 2000–2025 period, indicating a subtle basin-wide greening. This positive trend is modest in magnitude and spatially heterogeneous, consistent with the land-cover specific trends shown in Figure 6 (e.g., croplands display the most pronounced positive trend,  $\approx +0.0042$  NDVI units yr<sup>-1</sup>). However, medium-resolution analyses identify localized

areas of substantial decline (hotspots) that are masked by these basin-scale averages, allowing a basin-wide greening signal to coexist with severe local degradation.

This slight basin-wide greening occurs alongside a statistically significant increase in mean growing-season temperature (0.05 °C yr<sup>-1</sup>; p = 0.0102). Total growing-season precipitation, in contrast, shows pronounced inter-annual variability but does not exhibit a clear long-term directional trend over the analysis period.

The relationships between basin-wide annual vegetation indices and climatic factors were quantified using Pearson correlation (Figure 3). NDVI shows a moderate, statistically significant positive correlation with precipitation (r = 0.5017, p = 0.009), confirming moisture availability as an important driver of inter-annual vegetation variability. By contrast, the basin-wide correlation between NDVI and temperature is weak and not statistically significant (r = 0.0902, p = 0.6611). This spatial heterogeneity is evident in the pixel-wise correlation maps (Figure 5), which reveal moderate to strong positive NDVI—precipitation correlations in northern/rainfed areas and localized negative NDVI—temperature associations in irrigated southern plains.

The long-term MODIS time-series indicate a subtle basin-scale greening trend in NDVI and SAVI between 2000 and 2025, occurring concurrently with a statistically significant warming trend and strong inter-annual precipitation variability. However, because this greening is modest and spatially uneven, basin-scale averages alone can obscure critical local declines, a point that is directly addressed by the medium-resolution Landsat hotspot analysis in Section 3.3.

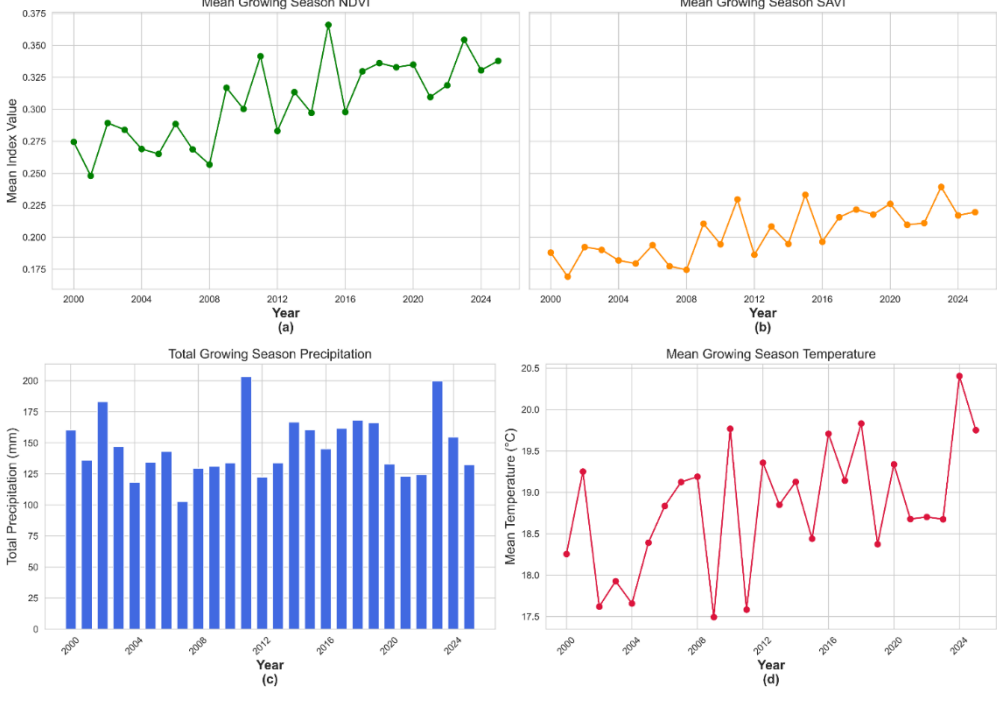


**Figure 2.** Basin-wide time series of key environmental variables in the Konya Basin during the growing season (2000–2025) derived from MODIS (NDVI/SAVI), CHIRPS (Precipitation), and ERA5-Land (Temperature) data: (a) annual mean NDVI, (b) annual mean SAVI, (c) total precipitation, and (d) mean temperature

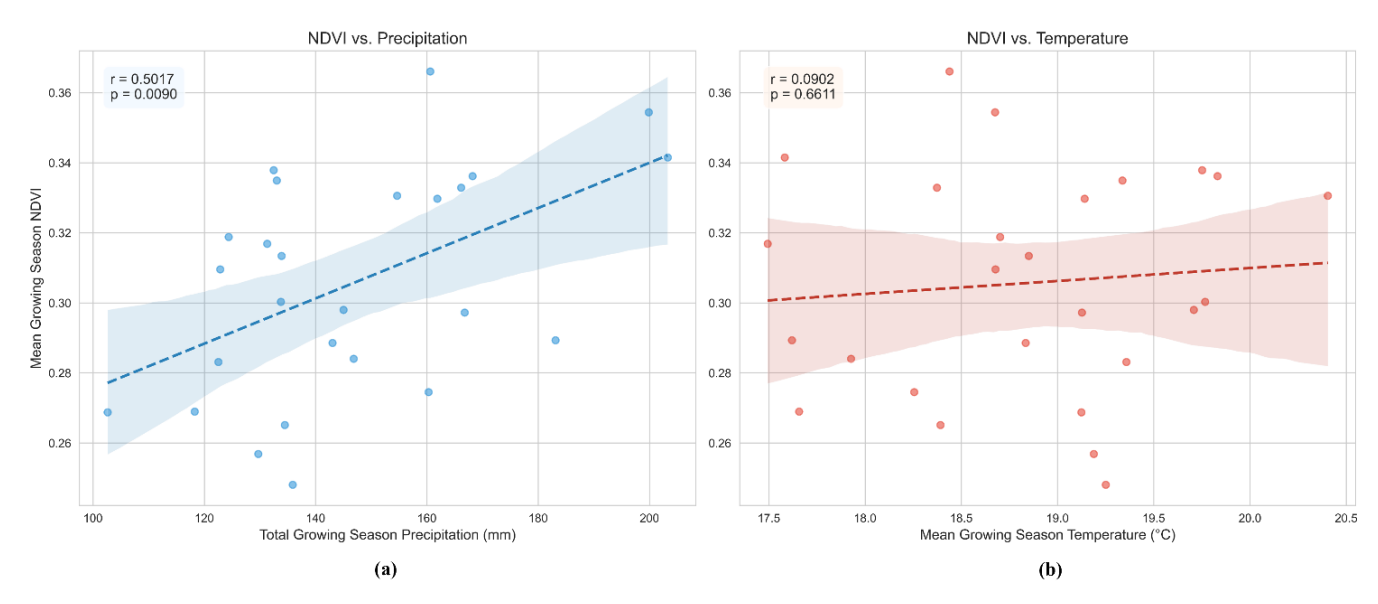


**Figure 3.** Relationships between basin-wide mean NDVI and climatic factors during the growing season (2000–2025): (a) NDVI vs. precipitation and (b) NDVI vs. temperature.

# 3.2 Spatial Patterns of Vegetation Change

The spatial analysis of vegetation dynamics reveals significant heterogeneity in degradation and greening patterns across the Konya Basin. The pixel-wise linear trend slopes for NDVI and SAVI are presented in Figure 4. Both indices show widespread areas of positive slopes (greening) across the basin, particularly in peripheral highland regions. Localized negative slopes (degradation) are concentrated in the central and southern plains where agricultural activities

dominate land use. The SAVI trend map closely mirrors these results.

The spatial correlation maps (Figure 5) further elucidate vegetation—climate interactions. A strong positive correlation between NDVI and precipitation is evident in the northern and peripheral grasslands, which are predominantly rainfed ecosystems. In contrast, correlations between NDVI and temperature are largely negative in the irrigated southern agricultural plains.

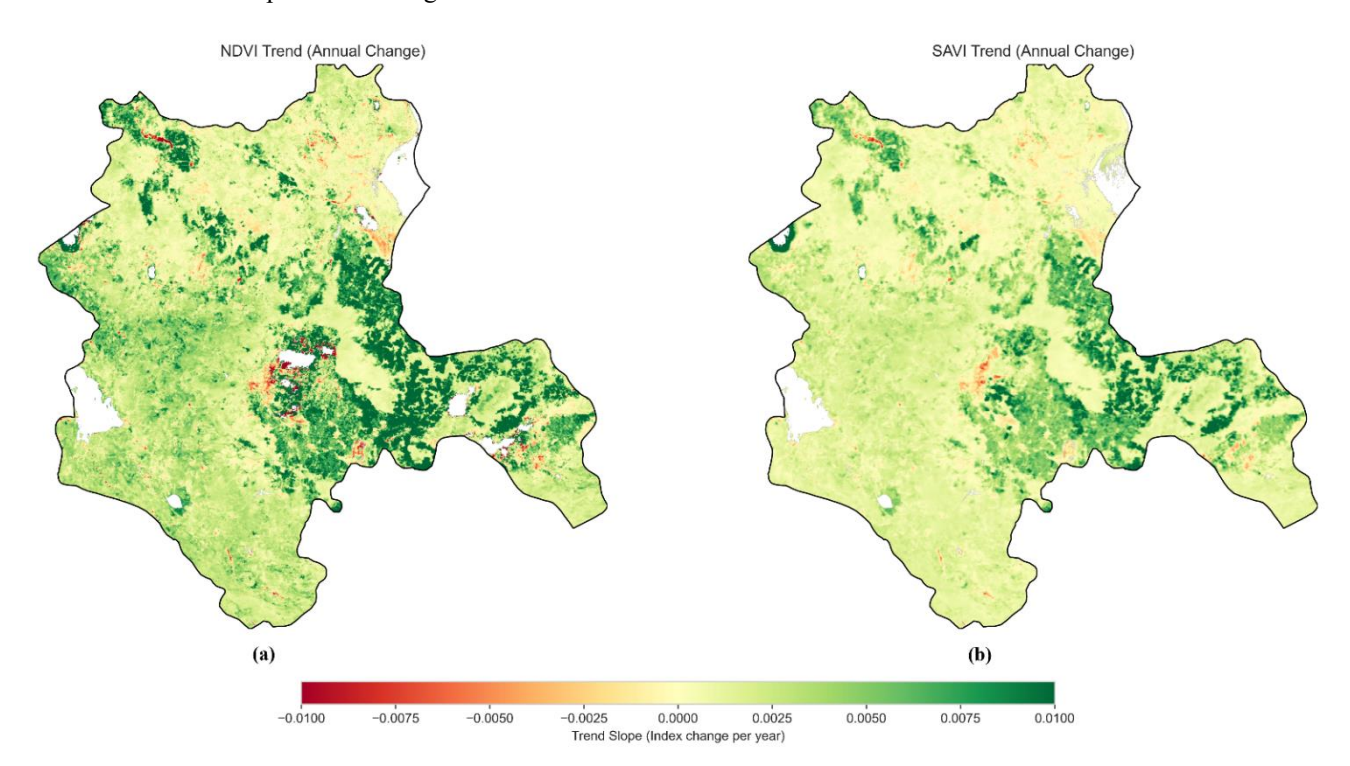


**Figure 4.** Spatial distribution of vegetation trends in the Konya Basin from 2000 to 2025 calculated from the MODIS (MOD13Q1 and MOD09A1) time-series: (a) NDVI trend slope and (b) SAVI trend slope.

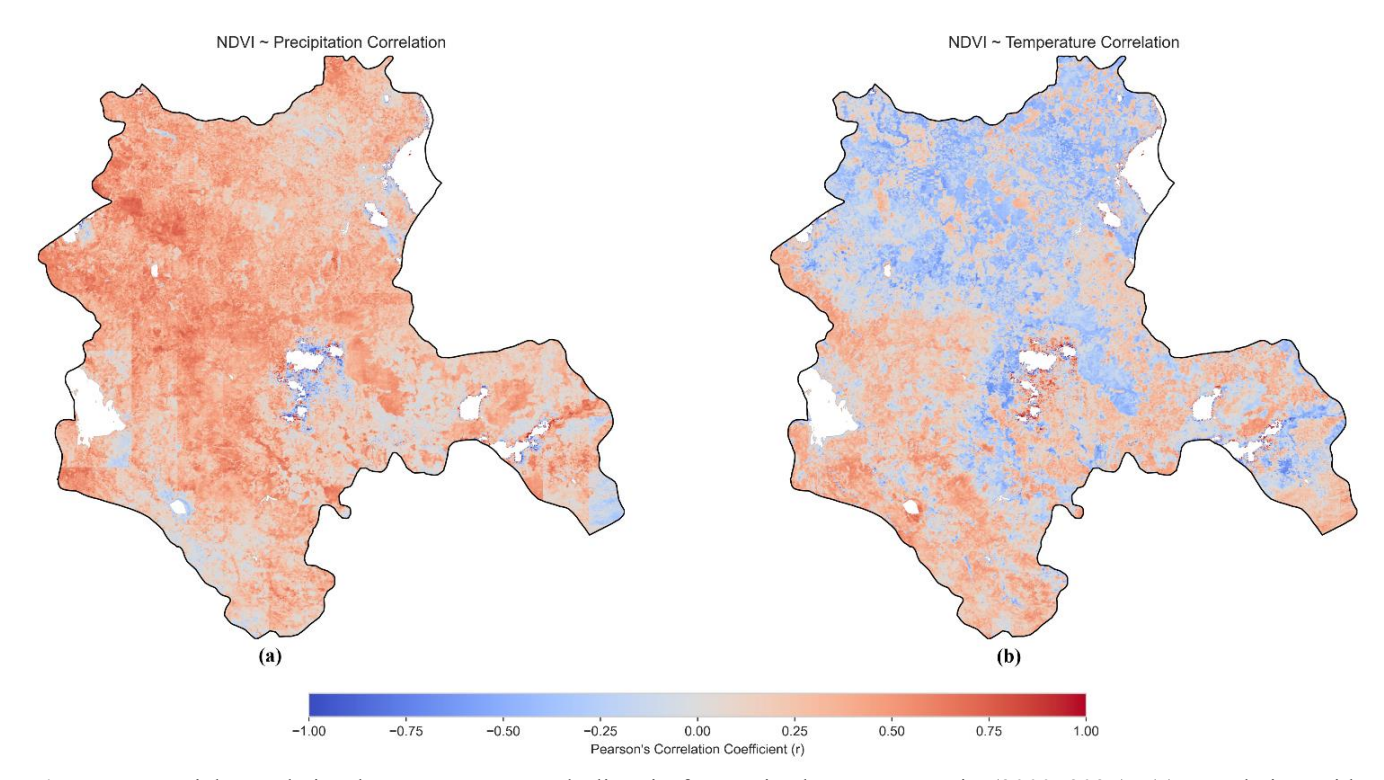


**Figure 5.** Spatial correlation between NDVI and climatic factors in the Konya Basin (2000–2025): (a) correlation with precipitation and (b) correlation with temperature.

The spatial trend and correlation analyses demonstrate that the Konya Basin exhibits a heterogeneous environmental dynamic: widespread but modest greening coexists with concentrated degradation hotspots. This spatial paradox underlines the importance of integrating basin-wide trends with fine-scale assessments to fully capture the desertification risk landscape.

# 3.3 Impact of Land Use and Medium-Resolution Degradation Hotspots

Land use emerges as a key factor shaping vegetation dynamics. As shown in Figure 6, cropland areas exhibit the most pronounced positive NDVI trend compared to grasslands and bare/sparse vegetation zones. This greening trend in croplands is consistent with the basin-wide increase of  $\approx +0.0042$  NDVI units yr<sup>-1</sup>. At the same time, medium-resolution analyses reveal that localized degradation persists, particularly within intensively managed agricultural zones.

The Landsat-based hotspot analysis provides a more detailed perspective on recent vegetation change, summarized in Table 2. A total of 3471.93 km² was identified as experiencing significant degradation between 2013–2015 and 2023–2025 [as described in Section 2.5]. Croplands account for 741.52 km² (21.4% of the total degraded area), grasslands for 168.92 km² (4.9%), and bare/sparse vegetation for 142.46 km² (4.1%).

The spatial distribution of these hotspots is visualized in Figure 7, demonstrating that vegetation decline is not randomly distributed but is concentrated in specific agricultural parcels and irrigation schemes, particularly in the southern and central plains.

These results indicate that widespread greening and concentrated degradation hotspots coexist within the Konya Basin, underscoring the importance of integrating basin-wide averages with medium-resolution analyses.

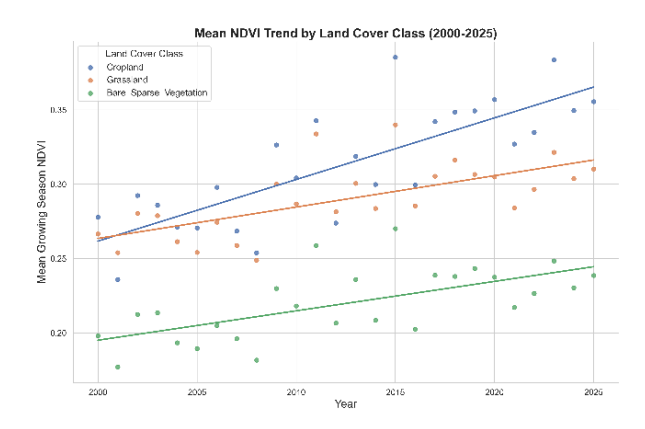


**Figure 6.** Trends in mean growing season NDVI (2000–2025), disaggregated by major land cover classes.

**Table 2.** Distribution of medium-resolution degradation hotspots across land cover classes in the Konya Basin.

Land Cover Class	Hotspot Area (km²)	Percentage of Total Hotspots (%)
Cropland	741.524	21.358
Grassland	168.919	4.865
Bare/Sparse Vegetation	142.461	4.103

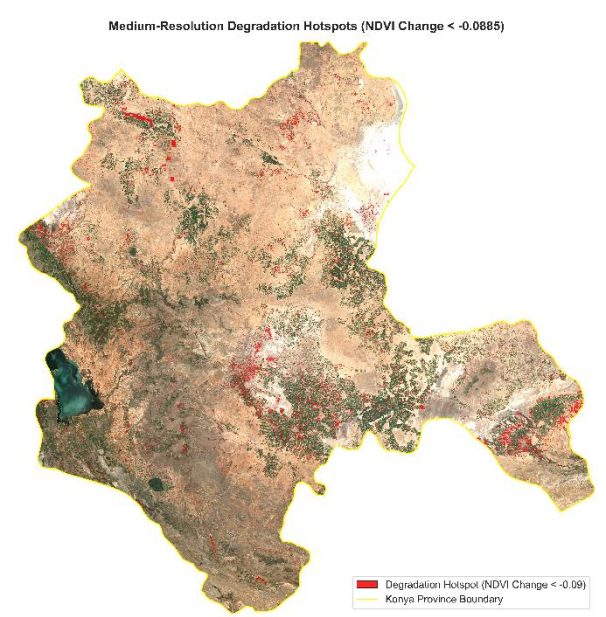


**Figure 7.** Spatial distribution of medium-resolution degradation hotspots identified using Landsat NDVI data for 2013–2025

# 3.4 Discussion

The results of this study provide compelling evidence of a complex environmental dynamic in the Konya Basin between 2000 and 2025. A subtle, basin-wide greening trend appears to mask acute, localized degradation that is driven by intensive agricultural activities. The spatial analyses reveal that while croplands exhibit the strongest positive long-term NDVI trend ( $\approx +0.0042$  units yr<sup>-1</sup>), they also contain a disproportionately high share of degradation hotspots (741.52 km²; 21.4% of the total). This apparent contradiction underscores the critical role of scale in vegetation monitoring: basin-wide averages suggest improvement, whereas medium-resolution data expose areas of severe decline.

The temporal analysis indicates a clear warming trend, with mean growing-season temperatures increasing by an average of  $0.05~^{\circ}\text{C}$  per year, statistically significant at p = 0.0102. This aligns with regional climate projections for Central Anatolia, which identify temperature rise as a primary driver of increased aridity [39, 40]. The basin-wide correlation analysis supports a complex relationship: NDVI showed a moderate positive correlation with precipitation (r = 0.5017, p = 0.009), confirming the region's dependence on moisture, while the basin-wide correlation with temperature was not statistically significant (r = 0.09, p = 0.66). However, spatial correlation maps clarified this discrepancy, revealing strong positive NDVI—precipitation relationships in northern rainfed areas and localized negative NDVI—temperature associations in irrigated southern croplands.

These findings suggest that the drivers of vegetation dynamics in the Konya Basin are heterogeneous. This dynamic is consistent with findings from other semi-arid regions in Turkey; for example, [41], in their study on land cover-temperature relationships in Kayseri, found that bare soil areas significantly increased land surface temperatures, providing a supporting framework for explaining the

temperature stress observed in the intensively cultivated agricultural plains of Konya. Rainfed ecosystems primarily respond to inter-annual precipitation variability, while irrigated croplands are more vulnerable to rising temperatures and unsustainable groundwater extraction. The identification of 3471.93 km² of severe degradation, concentrated in the southern and central plains and predominantly below 1000 m elevation, strongly supports this interpretation. This pattern indicates stress driven by unsustainable resource use, consistent with subsidence studies in semi-arid basins [42, 43].

The paradox of widespread greening coexisting with localized degradation has also been reported in other semi-arid regions, including the Sahel, Central Asia, and parts of China [44, 45]. In the Konya Basin, agricultural intensification and CO<sub>2</sub> fertilization may contribute to the observed basin-scale greening [46], while land and water management practices drive the emergence of degradation hotspots. This dual process illustrates why reliance on basin-wide NDVI averages alone can be misleading, as they conceal critical vulnerabilities in agricultural landscapes.

While this study provides a comprehensive remote sensing-based assessment, certain limitations must be acknowledged. The primary limitations are the spatial resolution mismatch between datasets and the use of a static land cover map. The coarse spatial resolution of climatic data (~5–11 km) averages temperature and precipitation over large areas, potentially masking localized microclimatic effects that influence vegetation at finer scales and thereby weakening the observed pixel-level correlations. Similarly, the use of a static 2020 land cover map for a 26-year analysis assumes no significant land use conversions, while the expansion of irrigated agriculture could have occurred, potentially leading to the misclassification of vegetation change drivers in some areas. Future research should aim to integrate medium-resolution climate models and historical land-use data to refine spatial analysis.

Furthermore, incorporating direct data on groundwater levels would allow for a quantitative link between water resource depletion and the observed degradation hotspots. Nevertheless, the spatially explicit identification of degradation hotspots, even within a context of subtle overall greening, provides valuable input for targeted land management interventions. This highlights the urgent need for sustainable water policies, such as groundwater monitoring and water-efficient irrigation practices, to mitigate desertification risks in this vital agricultural region.

# 4 Conclusion

This study provides a comprehensive, multi-sensor remote sensing analysis of vegetation dynamics in the Konya Basin from 2000 to 2025. The long-term MODIS record reveals a subtle but consistent basin-wide greening trend in NDVI and SAVI, with croplands showing the most pronounced positive slope ( $\approx +0.0042$  units yr<sup>-1</sup>). At the same time, medium-resolution Landsat analysis identified 3471.93 km² of severe degradation hotspots, of which 21.4% occur in croplands and approximately 70% are concentrated below 1000 m elevation, where groundwater-dependent

irrigation is most intensive. These findings demonstrate that apparent greening at the basin scale can mask critical local-scale degradation processes.

Climatic analysis indicates a statistically significant warming trend of  $0.05~^{\circ}\text{C}$  yr $^{-1}$  (p = 0.0102), while precipitation exerts strong inter-annual control on vegetation (r = 0.5017, p = 0.009). In contrast, the basin-wide NDVI-temperature relationship is weak and not statistically significant (r = 0.09, p = 0.66). Spatial correlation maps clarify this discrepancy, showing strong positive NDVI-precipitation relationships in northern rainfed grasslands and localized negative NDVI-temperature associations in irrigated southern plains. Together, these results confirm that vegetation responses are heterogeneous, with rainfed systems sensitive to precipitation variability and irrigated croplands highly vulnerable to warming and water stress.

The key scientific contribution of this research is the clear demonstration of the "greening–degradation paradox" in a semi-arid agro-ecosystem: modest basin-wide greening, partly driven by agricultural intensification and CO<sub>2</sub> fertilization, coexists with acute local degradation concentrated in irrigated agricultural zones. By integrating long-term MODIS trends with medium-resolution Landsat hotspot detection, this research provides robust evidence that basin-scale averages alone are insufficient to characterize desertification risk.

The results have significant implications for regional policy and sustainable resource management. The spatially explicit identification of degradation hotspots offers a valuable tool for decision-makers to shift from basin-wide strategies to targeted interventions. To enhance resilience, we recommend concrete policy actions, including (1) establishing a basin-wide network of telemetered wells for real-time groundwater monitoring, and (2) providing targeted subsidies to accelerate the transition from flood irrigation to modern drip or sprinkler systems. While providing a strong evidence base, this study acknowledges limitations such as the coarse resolution of climate data and the use of a static land cover map. Future studies incorporating dynamic land-use maps and groundwater data would further refine these findings and strengthen the evidence base for sustainable land and water management in the Konya Basin.

## Similarity (iThenticate): %10

#### References

- [1] UNCCD, United Nations Convention to Combat Desertification in Those Countries Experiencing Serious Drought and/or Desertification, Particularly in Africa, United Nations, 1994.

  https://www.unccd.int/sites/default/files/2022-02/UNCCD\_Convention\_ENG\_0.pdf
- [2] IPCC, Climate Change 2022 Impacts, Adaptation and Vulnerability: Working Group II Contribution to the Sixth Assessment Report of the Intergovernmental Panel on Climate Change. Cambridge: Cambridge University Press, 2023.
- [3] J. F. Reynolds, D. M. S. Smith, E. F. Lambin, B. Turner, M. Mortimore, S. P. Batterbury, T. R. Downing, H.

- Dowlatabadi, R. J. Fernández, J. E. Herrick, Global desertification: building a science for dryland development. Science, 316, 5826, 847-851, 2007. http://dx.doi.org/10.1126/science.1131634.
- [4] A. R. Huete, A Soil-Adjusted Vegetation Index (Savi). Remote Sens Environ, 25, 3, 295-309, 1988. https://doi.org/10.1016/0034-4257(88)90106-X.
- [5] E. Lioubimtseva, R. Cole, J. M. Adams, and G. Kapustin, Impacts of climate and land-cover changes in arid lands of Central Asia. J Arid Environ, 62, 2, 285-308, 2005. https://doi.org/10.1016/j.jaridenv.2004.11.005.
- [6] J. Peñuelas and M. Boada, A global change-induced biome shift in the Montseny mountains (NE Spain). Global change biology, 9, 2, 131-140, 2003. http://dx.doi.org/10.1046/j.1365-2486.2003.00566.x.
- [7] F. Alshehri, B. A. Abuamarah, and H. T. Abd El-Hamid, Impact of land use dynamics on land surface temperature using optical remote sensing data integrated with statistical analysis in Riyadh, Saudi Arabia. Advances in Space Research, 72, 5, 1739-1750, 2023. https://doi.org/10.1016/j.asr.2023.04.051.
- [8] M. H. Easdale, O. Bruzzone, P. Mapfumo, and P. Tittonell, Phases or regimes? Revisiting NDVI trends as proxies for land degradation. Land Degradation & Development, 29, 3, 433-445, 2018. https://doi.org/10.1002/ldr.2871.
- [9] G. Faour, M. Mhawej, and A. Fayad, Detecting changes in vegetation trends in the Middle East and North Africa (MENA) region using SPOT vegetation. Cybergeo: European Journal of Geography, 2016. https://doi.org/10.4000/cybergeo.27620.
- [10] S. W. Rifai, M. G. De Kauwe, A. M. Ukkola, L. A. Cernusak, P. Meir, B. E. Medlyn, A. J. Pitman, Thirty-eight years of CO<sup>2</sup> fertilization have outpaced growing aridity to drive greening of Australian woody ecosystems. Biogeosciences Discussions, 2021, 1-41, 2021. https://doi.org/10.5194/bg-19-491-2022.
- [11] P. Gonzalez, C. J. Tucker, and H. Sy, Tree density and species decline in the African Sahel attributable to climate. J Arid Environ, 78, 55-64, 2012. https://doi.org/10.1016/j.jaridenv.2011.11.001.
- [12] S. Piao, X. Wang, T. Park, C. Chen, X. Lian, Y. He, J. W. Bjerke, A. Chen, P. Ciais, H. Tømmervik, Characteristics, drivers and feedbacks of global greening. Nature Reviews Earth & Environment, 1, 1, 14-27, 2020. http://dx.doi.org/10.1038/s43017-019-0001-x.
- [13] C. Chen, T. Park, X. Wang, S. Piao, B. Xu, R. K. Chaturvedi, R. Fuchs, V. Brovkin, P. Ciais, R. Fensholt, H. Tømmervik, G. Bala, Z. Zhu, R. R. Nemani, R. B. Myneni, China and India lead in greening of the world through land-use management. Nature sustainability, 2, 2, 122-129, 2019. https://www.nature.com/articles/s41893-019-0220-7.
- [14] O. Orhan, M. Haghshenas Haghighi, V. Demir, E. Gökkaya, F. Gutiérrez, and D. Al-Halbouni, Spatial and temporal patterns of land subsidence and sinkhole occurrence in the Konya Endorheic Basin, Turkey.

- Geosciences, 14, 1, 5, 2023. https://doi.org/10.3390/geosciences14010005.
- [15] O. Orhan and M. Yakar, Investigating land surface temperature changes using Landsat data in Konya, The International Archives Photogrammetry, Remote Sensing and Spatial 41. 285-289. Information Sciences. 2016. http://dx.doi.org/10.5194/isprsarchives-XLI-B8-285-2016.
- [16] F. Caló, D. Notti, J. P. Galve, S. Abdikan, T. Görüm, A. Pepe, F. Balık Şanlı, Dinsar-Based detection of land subsidence and correlation with groundwater depletion in Konya Plain. Turkey, Remote sensing, 9, 1, 83, 2017. https://doi.org/10.3390/rs9010083.
- [17] A. Çağlar, O. Dengiz, and I. Cinkaya, Monitoring of drought severity in Konya closed basin using Standardized Precipitation index and Modis satellite images. International Symposium on Soil Science and Plant Nutrition Samsun TÜRKİYE, 18-19 December 2021.
- [18] V. Kartal and M. Nones, Assessment of meteorological, hydrological and groundwater drought in the Konya closed basin, Türkiye. Environmental Earth Sciences, 83, 9, 285, 2024/05/02 2024. https://doi.org/10.1007/s12665-024-11587-1.
- [19] N. Yagmur, B. B. Bilgilioglu, N. Musaoglu, E. Erten, and A. Tanik, Temporal changes of lentic system surfaces in Konya Closed Basin, Turkey. Conference Proceeding Book: 3rd International Conference on Civil and Environmental Engineering (ICOCEE), Çeşme Türkiye, 24-27 April 2018.
- [20] G. Yılmaz, M. A. Çolak, İ. K. Özgencil, M. Metin, M. Korkmaz, S. Ertuğrul, M. Soyluer, T. Bucak, Ü. N. Tavşanoğlu, K. Özkan, Z. Akyürek, M. Beklioğlu, E. Jeppesen, Decadal changes in size, salinity, waterbirds, and fish in lakes of the Konya Closed Basin, Turkey, associated with climate change and increasing water abstraction for agriculture. Inland Waters, 11, 4, 538-555, 2021. https://doi.org/10.1080/20442041.2021.1924034.
- [21] S. Abdikan, A. Sekertekin, M. Ustuner, F. Balik Sanli, and R. Nasirzadehdizaji, Backscatter analysis using multi-temporal Sentinel-1 SAR data for crop growth of maize in Konya Basin, Turkey. *The International Archives of the Photogrammetry, Remote Sensing and Spatial Information Sciences*, 42, 9-13, 2018. http://dx.doi.org/10.5194/isprs-archives-XLII-3-9-2018.
- [22] F. Calò, D. Notti, J. Galve, S. Abdikan, T. Görüm, O. Orhan, H. B. Makineci, A. Pepe, M. Yakar, F. Balik Şanlı, A multi-source data approach for the investigation of land subsidence in the Konya basin, Turkey. The International Archives of Photogrammetry, Remote Sensing and Spatial 42, 129-135, Information Sciences, 2018. https://doi.org/10.5194/isprs-archives-XLII-3-W4-129-2018.
- [23] N. Şireci, G. Aslan, and Z. Cakir, Long-term spatiotemporal evolution of land subsidence in Konya

- metropolitan area (Turkey) based on multisensor SAR data. Turkish Journal of Earth Sciences, 30, 5, 681-697, 2021. https://doi.org/10.3906/yer-2104-22.
- [24] K. M. de Beurs and G. M. Henebry, A statistical framework for the analysis of long image time series. International Journal of Remote Sensing, 26, 8, 1551-1573, 2005. http://dx.doi.org/10.1080/01431160512331326657.
- [25] K. M. de Beurs, C. K. Wright, and G. M. Henebry, Dual scale trend analysis for evaluating climatic and anthropogenic effects on the vegetatedland surface in Russia and Kazakhstan. Environmental Research Letters, 4, 4, 045012, 2009. http://dx.doi.org/10.1088/1748-9326/4/4/045012.
- [26] H. Eskandari Dameneh, H. Gholami, M. W. Telfer, J. R. Comino, A. L. Collins, and J. D. Jansen, Desertification of Iran in the early twenty-first century: assessment using climate and vegetation indices. Scientific Reports, 11, 1, 20548, 2021. https://doi.org/10.1038/s41598-021-99636-8.
- [27] IPCC, Climate Change and Land: an IPCC special report on climate change, desertification, land degradation, sustainable land management, food security, and greenhouse gas fluxes in terrestrial ecosystems, 2019.
- [28] A. W. Ahmed, E. Kalkan, A. Guzy, M. Alacali, and A. Malinowska, Modeling of land subsidence caused by groundwater withdrawal in Konya Closed Basin, Turkey. Proceedings of the International Association of Hydrological Sciences, 382, 397-401, 2020. https://doi.org/10.5194/piahs-382-397-2020.
- [29] M. Mayes, E. Marin-Spiotta, L. Szymanski, M. A. Erdoğan, M. Ozdoğan, and M. Clayton, Soil type mediates effects of land use on soil carbon and nitrogen in the Konya Basin, Turkey. Geoderma, 232, 517-527, 2014. https://doi.org/10.1016/j.geoderma.2014.06.002.
- [30] N. Gorelick, M. Hancher, M. Dixon, S. Ilyushchenko, D. Thau, and R. Moore, Google Earth Engine: Planetary-scale geospatial analysis for everyone. Remote Sens Environ, 202, 18-27, 2017. https://doi.org/10.1016/j.rse.2017.06.031.
- [31] K. Didan, MOD13Q1 MODIS/Terra vegetation indices 16-day L3 global 250m SIN grid V006. NASA EOSDIS Land Processes Distributed Active Archive Center (DAAC) data set, MOD13Q1. 006, 2015.
- [32] USGS. Landsat 8-9 Collection 2 Level-2 Science Products. https://www.usgs.gov/landsat-missions/landsat-collections Accessed 10 June 2025.
- [33] C. Funk, P. Peterson, M. Landsfeld, D. Pedreros, J. Verdin, S. Shukla, G. Husak, J. Rowland, L. Harrison, A. Hoell, The climate hazards infrared precipitation with stations—a new environmental record for monitoring extremes. Scientific data, 2, 1, 1-21, 2015. https://doi.org/10.1038/sdata.2015.66.
- [34] J. Muñoz-Sabater, E. Dutra, A. Agustí-Panareda, C. Albergel, G. Arduini, G. Balsamo, S. Boussetta, M. Choulga, S. Harrigan, H. Hersbach, ERA5-Land: A state-of-the-art global reanalysis dataset for land

- applications. Earth system science data, 13, 9, 4349-4383, 2021. https://doi.org/10.24381/cds.68d2bb30.
- [35] D. Zanaga, R. Van De Kerchove, D. Daems, W. De Keersmaecker, C. Brockmann, G. Kirches, J. Wevers, O. Cartus, M. Santoro, S. Fritz, ESA WorldCover 10 m 2021. v200, 2022. https://doi.org/10.5281/zenodo.7254221.
- [36] T. G. Farr, P. A. Rosen, E. Caro, R. Crippen, R. Duren, S. Hensley, M. Kobrick, M. Paller, E. Rodriguez, L. Roth, The shuttle radar topography mission. Reviews of geophysics, 45, 2, 2007. https://doi.org/10.1029/2005RG000183.
- [37] C. J. Tucker, Red and photographic infrared linear combinations for monitoring vegetation. Remote Sens Environ, 8, 2, 127-150, 1979. https://doi.org/10.1016/0034-4257(79)90013-0.
- [38] J. W. Rouse Jr, R. H. Haas, D. Deering, J. Schell, and J. C. Harlan, Monitoring the vernal advancement and retrogradation (green wave effect) of natural vegetation. NASA 1974. https://ntrs.nasa.gov/citations/19750020419
- [39] T. B. Altın, B. Barak, and B. N. Altın, Change in precipitation and temperature amounts over three decades in central Anatolia, Turkey. Atmospheric and Climate Sciences, 2, 1, 107-125, 2012. http://dx.doi.org/10.4236/acs.2012.21013.
- [40] E. Ergene, F. Bektaş Balçık, and F. Balik Şanlı, Trends analysis of agricultural drought in central anatolian basin, Turkey. The International Archives of the Photogrammetry, Remote Sensing and Spatial Information Sciences, 48, 141-148, 2024. https://doi.org/10.5194/isprs-archives-XLVIII-4-W9-2024-141-2024.

- [41] M. H. Kesikoglu, C. Ozkan, and T. Kaynak, The impact of impervious surface, vegetation, and soil areas on land surface temperatures in a semi-arid region using Landsat satellite images enriched with Ndaisi method data. Environmental Monitoring and Assessment, 193, 3, 143, 2021. https://doi.org/10.1007/s10661-021-08916-3.
- [42] A. Üstün, E. Tuşat, S. Yalvaç, İ. Özkan, Y. Eren, A. Özdemir, İ.Ö. Bildirici, T. Üstüntaş, O. S. Kırtıloğlu, M. Mesutoğlu, Land subsidence in Konya Closed Basin and its spatio-temporal detection by GPS and DInSAR. Environmental earth sciences, 73, 10, 6691-6703, 2015. https://doi.org/10.1007/s12665-014-3890-5.
- [43] A. Bozdağ, Z. Ünal, A. E. Karkınlı, A. B. Soomro, M. S. Mir, and Y. Gulzar, An Integrated Approach for Groundwater Potential Prediction Using Multi-Criteria and Heuristic Methods. Water, 17, 8, 1212, 2025. https://doi.org/10.3390/w17081212.
- [44] S. Robinson, Land degradation in Central Asia: evidence, perception and policy. in The End of Desertification? Disputing Environmental Change in the Drylands: Springer, 451-490, 2016.
- [45] T. Berdimbetov, Z.-G. Ma, S. Shelton, S. Ilyas, and S. Nietullaeva, Identifying land degradation and its driving factors in the Aral sea basin from 1982 to 2015. Frontiers in Earth Science, 9, 2021. https://doi.org/10.3389/feart.2021.690000.
- [46] R. J. Donohue, M. L. Roderick, T. R. McVicar, and G. D. Farquhar, Impact of CO<sup>2</sup> fertilization on maximum foliage cover across the globe's warm, arid environments. Geophysical Research Letters, 40, 12, 3031-3035, 2013. https://doi.org/10.1002/grl.50563.

